

POLARIZATION OF LIGHT BACKSCATTERED BY WAVELENGTH-SCALE PARTICLES

KARRI MUINONEN,^{a,b*} JANI TYYNELÄ,^a EVGENIJ ZUBKO,^{a,c} HANNAKAISA LINDQVIST,^a
ANTTI PENTTILÄ,^a TUOMO PIENILUOMA,^a AND GORDEN VIDEEN^d

(Invited paper)

ABSTRACT. We analyze angular dependencies of light scattered by wavelength-scale particles into the backscattering regime, that is, into scattering angles $\theta \geq 90^\circ$. We consider spherical and cubic particles, oblate and prolate spheroidal particles, as well as clusters of spherical particles, all with equal-volume-sphere size parameters $4 \leq x \leq 10$ and real-valued refractive indices $1.1 \leq m \leq 2.0$. We offer interference-based explanations for the angular dependencies of the scattered intensity, degree of linear polarization for unpolarized incident light, and the depolarization ratio.

1. Introduction

Wavelength-scale small particles are known to exhibit three specific features near backscattering (e.g., [1] and references therein): the scattered intensity shows a backscattering peak; the degree of linear polarization for unpolarized incident light is negative; and the depolarization ratio is double-lobed. In what follows, some general characteristics of polarization are unveiled in the backscattering regime, allowing for the explanation of the aforescribed features and enabling the utilization of polarization as a means for retrieving sizes, shapes, and optical properties of the scattering particles.

In Sect. 2, we describe the numerical scattering computations for the particles, and, in Sect. 3, we discuss the interpretation of the computations. Sect. 4 includes the conclusions of the present study.

2. Scattering by wavelength-scale particles

We have carried out a systematic study of the angular scattering properties for spherical and cubic particles, oblate (aspect ratio 1.40) and prolate spheroidal particles (aspect ratio 0.71), as well as for a specific cluster of four spherical particles (Fig. 1). We have utilized the discrete-dipole approximation for the cubic particles, the T -matrix method for the spheroidal particles, and the Superposition T -matrix method for the clusters of spherical particles (for more details and references, see [1]).

For example, Figure 2 shows the angular scattering characteristics for a randomly oriented prolate spheroidal particle with equal-volume-sphere size parameters $x = 5, 7, \text{ and } 9$

as a function of the refractive index m : we depict the components of the scattered intensity parallel (I_{\parallel}) and perpendicular to the scattering plane (I_{\perp}), the degree of linear polarization for unpolarized incident light ($P = -S_{12}/S_{11}$, $S_{11} = I_{\parallel} + I_{\perp}$ and $S_{12} = I_{\parallel} - I_{\perp}$), and the depolarization ratio ($D = 1 - S_{22}/S_{11}$).

The systematic computations in Fig. 2 indicate vertical structure that is largely independent of the refractive index. This structure becomes slightly smeared for the degree of linear polarization but shows up clearly for the depolarization ratio. Similar structures are also seen for the other types of particles. Additional structure becomes evident when plotting the angular dependencies as a function of size parameter for a fixed refractive index.

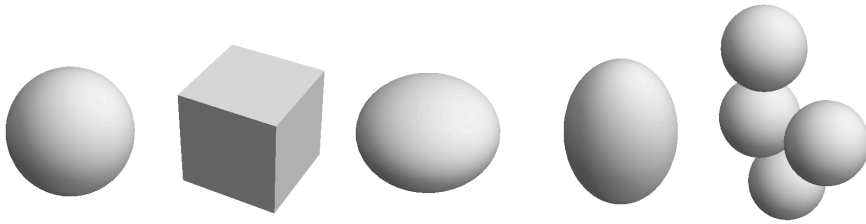


Figure 1. Shapes of wavelength-scale particles studied.

3. Discussion

In order to explain the angular dependencies partly shown in Fig. 2, consider the integration of a plane-wave internal field (wave number mk) over the volume of a spherical particle (high-energy approximation). The sequences of destructive ($N = n + \frac{1}{2}$, $n = 1, 2, \dots$) and constructive interferences ($N = n$, $n = 1, 2, \dots$) follow the rules expressed both for x and m as [1, 2]

$$x \approx \sqrt{\frac{N^2\pi^2 - 2}{m^2 + 1 - 2m \cos \theta}}, \quad m \approx \cos \theta + \sqrt{\cos^2 \theta + \frac{N^2\pi^2 - 2}{x^2} - 1}. \quad (1)$$

These rules show up clearly when plotting the angular dependencies for fixed m as a function of x [1].

Consider next a potential explanation for the vertical characteristics in Fig. 2. For wavelength-scale spherical particles, the internal fields exhibit wave patterns where the wavelength changes from the material wavelength near the central intersection line through the particle to match the external wavelength close to the particle boundary (to allow for the boundary conditions to be fulfilled). As a result, near the particle boundary in the interior, there is a regular placement of interference maxima and minima forming a standing-wave pattern so that the number of the maxima or minima is directly the same as the size parameter of the spherical particle, $x = 2\pi a/\lambda$. The regularity of the internal fields results in

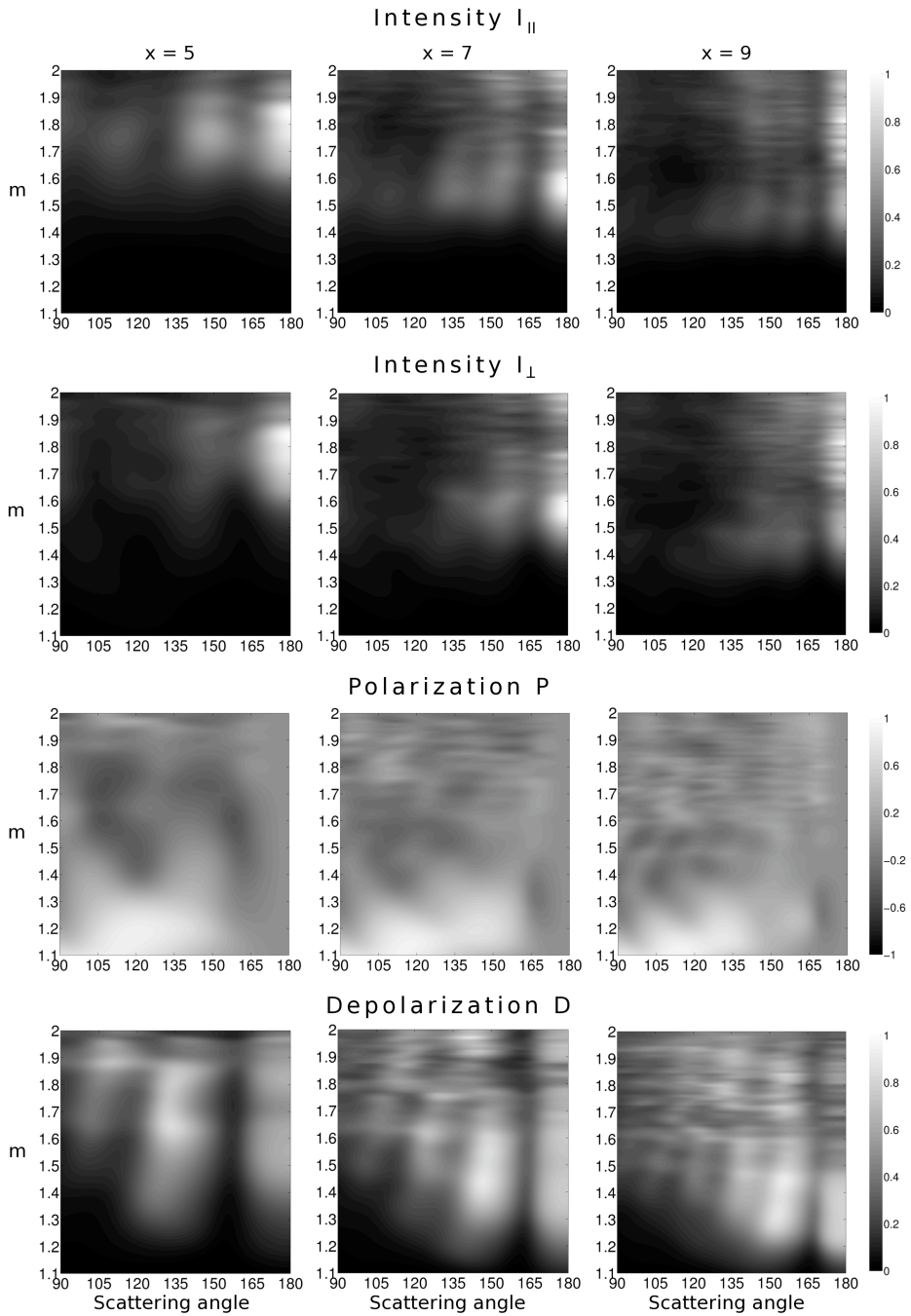


Figure 2. Angular scattering characteristics for a randomly oriented prolate spheroidal particle. See text.

what can be termed “an interference dial” for the mapping to the scattered field: rotating the dial by an angle corresponding to a quarter of the external wavelength ($\lambda/4$) on the perimeter accurately reproduces the constructive and destructive interference features in the angular patterns in most of the cases. At each quarter-wave rotation of the dial, there is either pairwise cancellation (destructive interference) or pairwise enhancement (constructive interference) of the contributions from various locations inside the scattering particle. The sequences of destructive ($N = n + \frac{1}{2}$, $n = 0, 1, 2, \dots$) and constructive interferences ($N = n$, $n = 0, 1, 2, \dots$) are given by the following straightforward rules for x , θ (scattering angle), and $\alpha = \pi - \theta$ (phase angle):

$$x \approx \frac{N\pi}{\pi - \theta} = \frac{N\pi}{\alpha}, \quad \theta \approx \pi - \frac{N\pi}{x}, \quad \alpha \approx \frac{N\pi}{x}. \quad (2)$$

These rules compare favorably with the vertical structure seen in Fig. 2.

Kerker [3] describes extensive analyses of size dependencies, where the locations of the interference features near forward scattering are documented using the function $(2a/\lambda) \sin(\theta/2)$ (cf. Eq. 1 for $m = 1$). We can conclude that, in the backscattering regime, it is more practical to utilize the rules in Eqs. 1-2.

In our earlier work [4], we have explained the negative polarization at intermediate scattering angles as resulting from localized longitudinal internal field components interfering constructively with each other. These internal-field components are accurately at opposite phase and are located half an external wavelength from one another close to the particle perimeter in the forward part of the interior. This picture is in full agreement with the aforescribed interference dial.

4. Conclusion

We have described systematic light-scattering computations for spherical and nonspherical particles and explained the resulting angular scattering characteristics in the backscattering regime as resulting from interference between contributions from different parts of the particle interiors. We will compare the present results to those for finite spherical scattering media significantly larger than the wavelength and composed of small spherical particles (see [5]).

References

- [1] K. Muinonen, J. Tyynelä, E. Zubko, H. Lindqvist, A. Penttilä, and G. Videen, “Polarization of light backscattered by small particles”, *JQSRT*, in press (2011).
- [2] C. F. Bohren and D. R. Huffman, “Absorption and Scattering of Light by Small Particles” (John Wiley & Sons, New York, 1983).
- [3] M. Kerker, “The Scattering of Light and Other Electromagnetic Radiation” (Academic Press, New York, 1969).
- [4] J. Tyynelä, E. Zubko, K. Muinonen, and G. Videen, “Interpretation of single-particle negative polarization at intermediate scattering angles”, *Appl. Opt.* **49**, 5284-5296 (2010).
- [5] Muinonen, K., and Zubko, E., “Coherent backscattering by a finite medium of particles”, in *Electromagnetic & Light Scattering XII, Conference Proceedings*; Helsinki, Finland, 2010; K. Muinonen, A. Penttilä, H. Lindqvist, T. Nousiainen, and G. Videen, Eds., pp. 194-197.

^a University of Helsinki
Department of Physics
P.O. Box 64
FI-00014 U. Helsinki, Finland

^b Finnish Geodetic Institute
Geodeetinrinne 2, P.O. Box 15
FI-02431 Masala, Finland

^c Kharkov National University
Institute of Astronomy
35 Sumskaya St.
Kharkov, 61022, Ukraine

^d Army Research Laboratory
2800 Powder Mill Rd.
Adelphi
Maryland 20783, U.S.A.

* To whom correspondence should be addressed | Email: karri.muinonen@helsinki.fi

Paper presented at the ELS XIII Conference (Taormina, Italy, 2011), held under the APP patronage; published online 15 September 2011.

© 2011 by the Author(s); licensee *Accademia Peloritana dei Pericolanti*, Messina, Italy. This article is an open access article, licensed under a [Creative Commons Attribution 3.0 Unported License](#).